Supplementary Figure 18

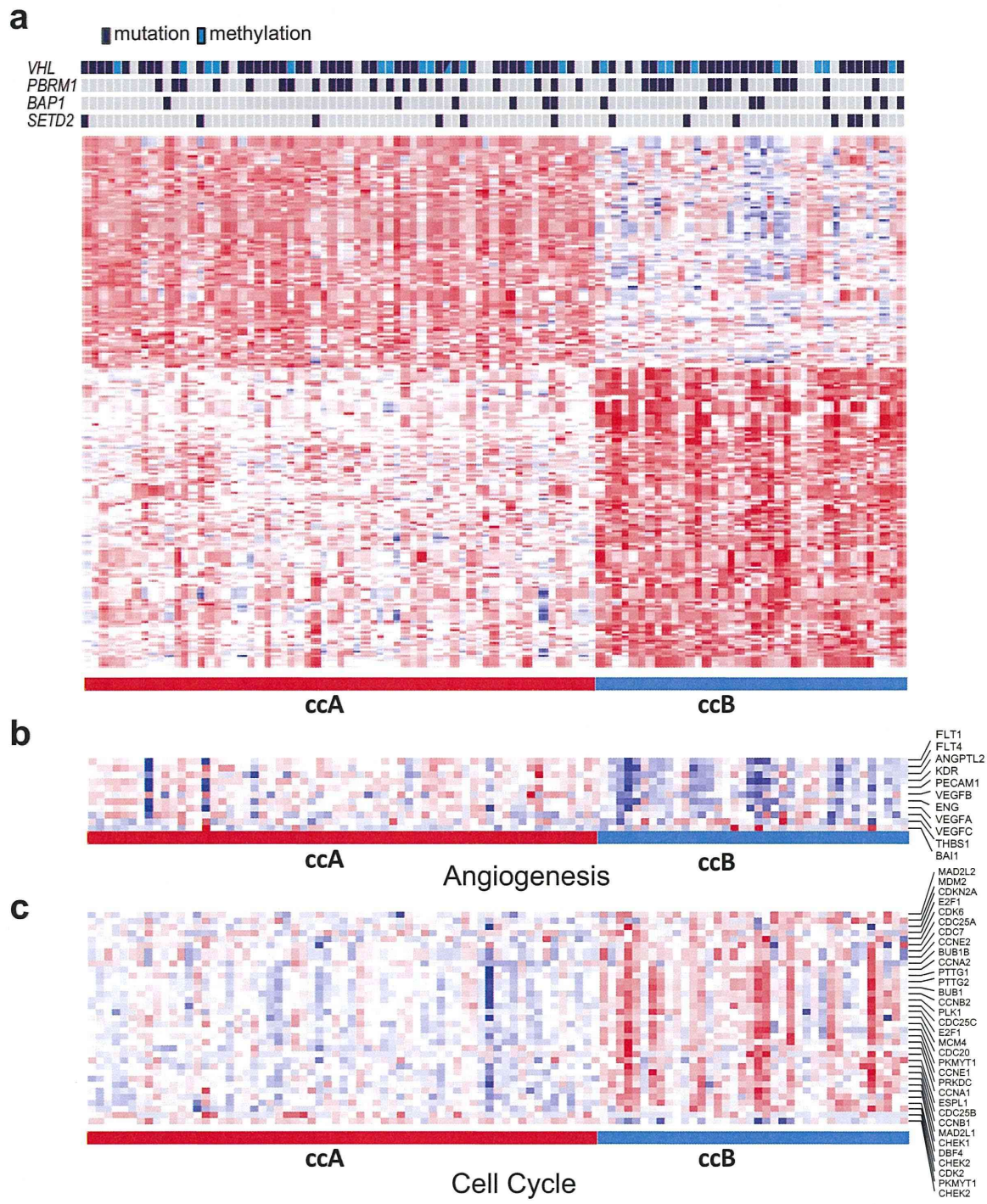

ccA and ccB clusters identified from the expression profiles of 101 ccRCC samples
K-means clustering for 101 ccRCC specimens based on the expression of genes showing 2 major gene expression clusters: ccA and ccB (**a**). These were discriminated by the expression of genes involved in angiogenesis (**b**) and cell cycle progression (**c**). Mutation status of *VHL, PBRM1, BAP1* and *SETD2* is indicated in the top panels.

Nature Genetics: doi:10.1038/ng.2699

Supplementary Figure 19

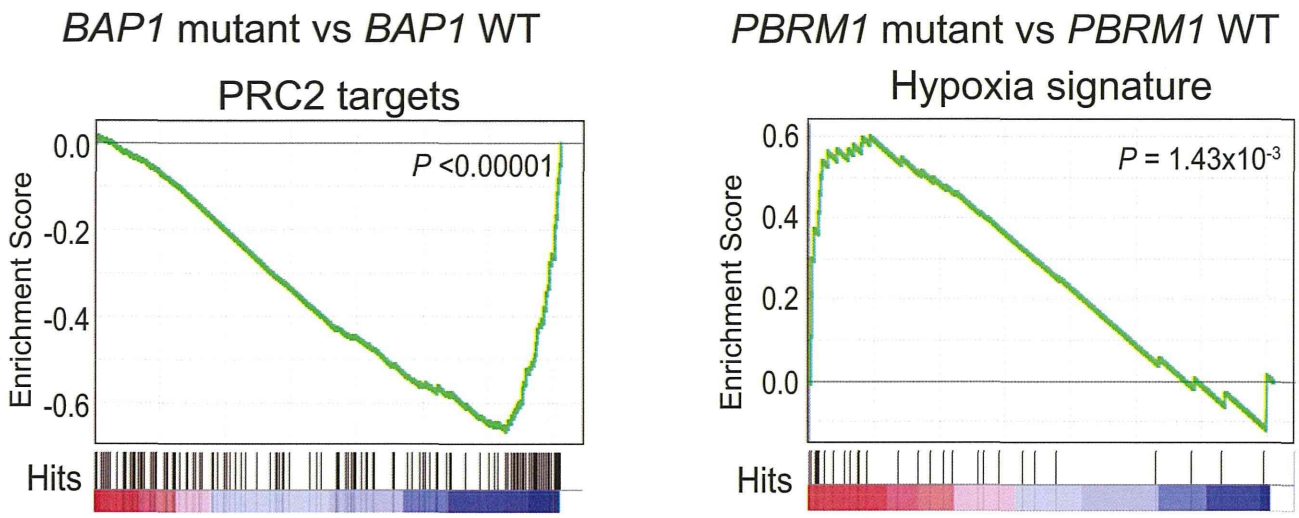

Different expression signatures between *BAP1*- and *PBRM1*-mutated tumors. Gene set enrichment analysis showed *BAP1*-mutated tumors showed significantly down-regulated expression of the PRC2 target genes, whereas *PBRM1*-mutated tumors were enriched for an up-regulated expression of gene set of hipoxia signature.

Supplementary Figure 20

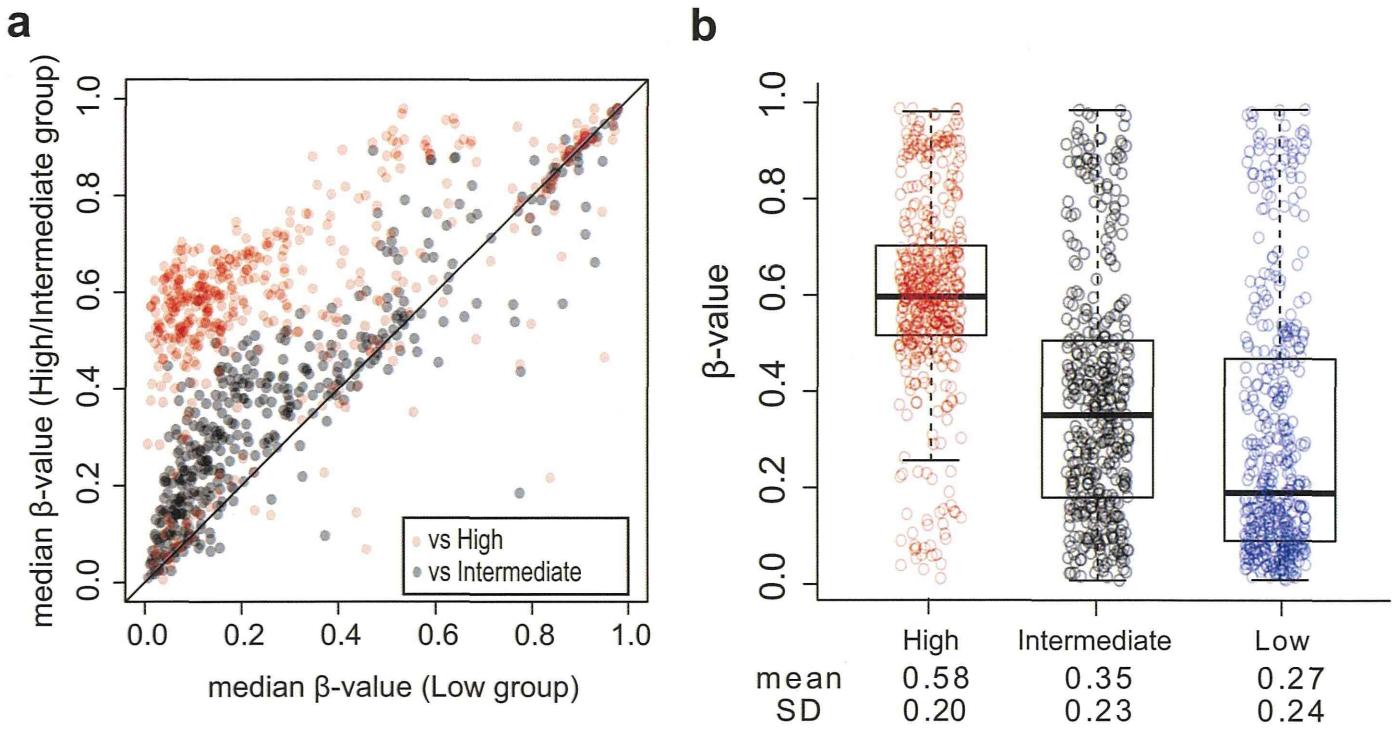

Difference of methylation level among high/intimidate/low methylation clusters
(**a**) Median methylation levels (β values) are plotted for Low and High (red circles) and Low and Intermediate (black circles) methylation clusters for CpG island probes selected for unsupervised clustering analysis in Infinium 450K arrays. (**b**) Distribution of median methylation values (β values) are plotted within each methylation cluster (High, Intermediate and Low).

Nature Genetics: doi:10.1038/ng.2699

Supplementary Figure 21

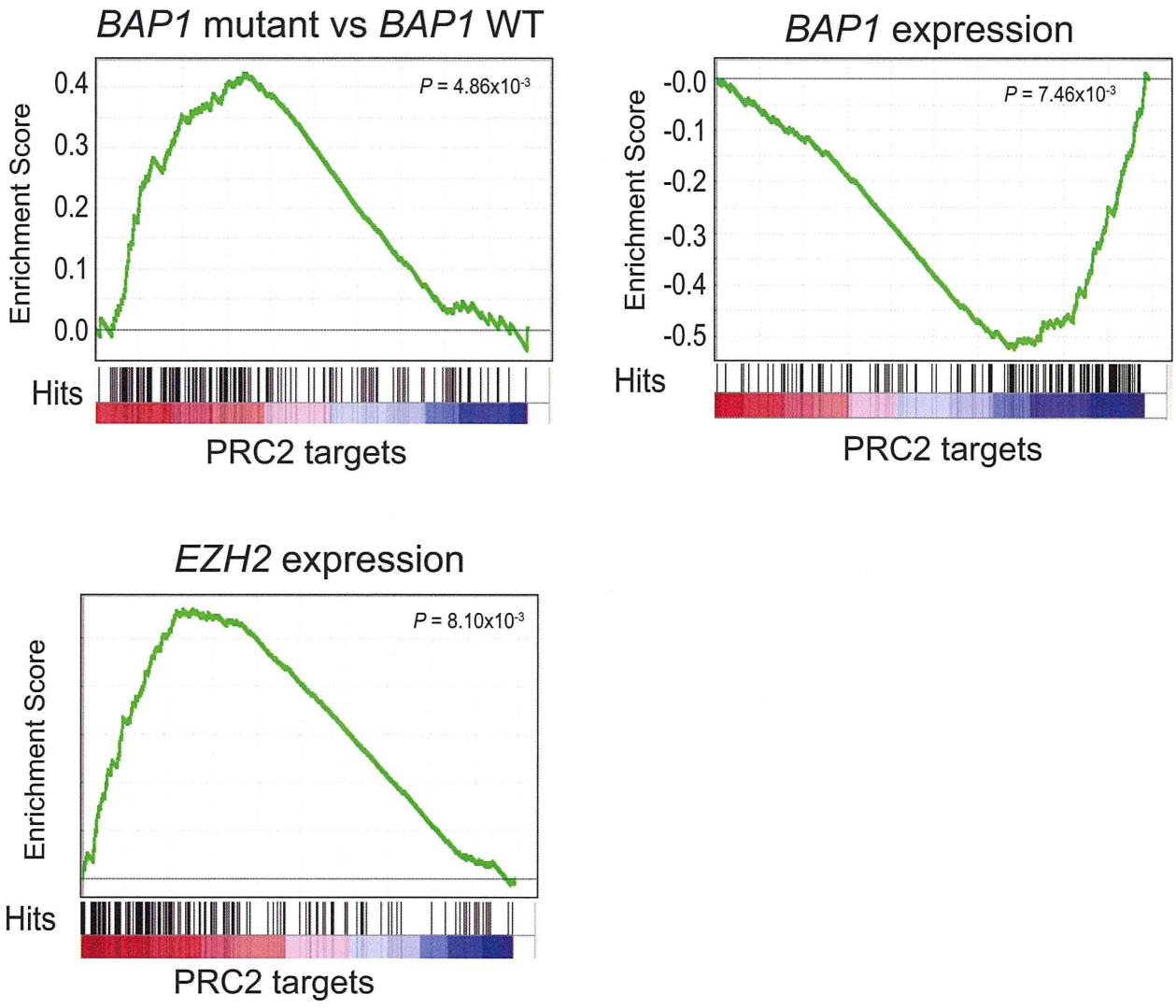

Association between methylation of PRC2 target genes and *BAP1* mutation/expression and *EZH2* expression

Gene set enrichment analysis showed *BAP1* mutation, decreased *BAP1* expression and increased *EZH2* expression were significantly associated with increased methylation of PRC2 target genes.

Nature Genetics: doi:10.1038/ng.2699

Supplementary Figure 22

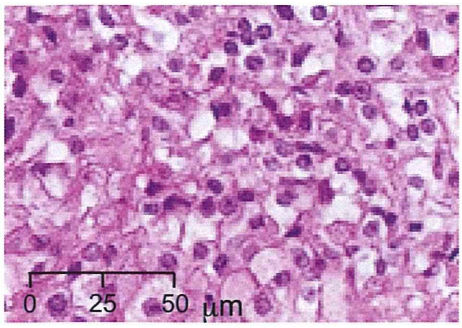

ccRCC-2

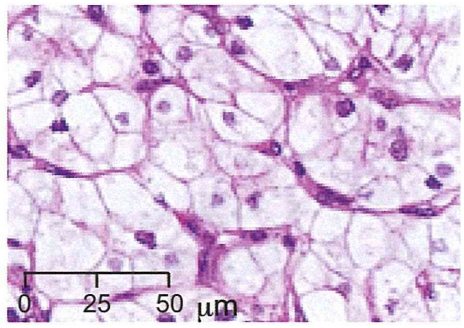

ccRCC-31

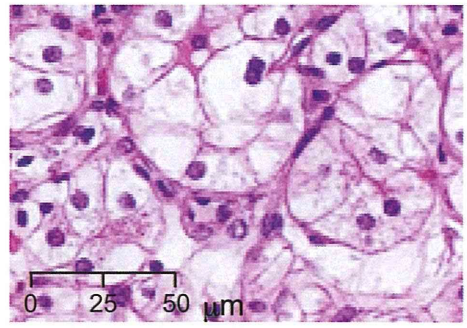

ccRCC-37

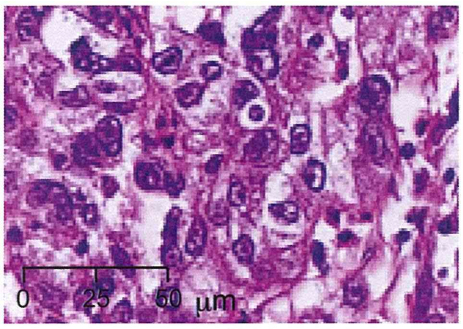

ccRCC-41

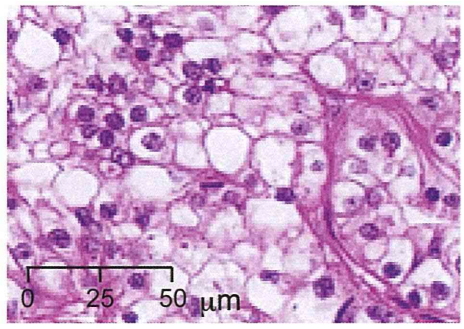

ccRCC-57

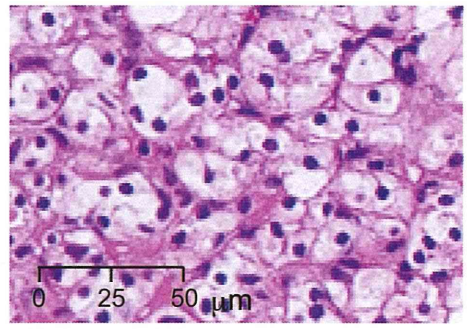

ccRCC-60

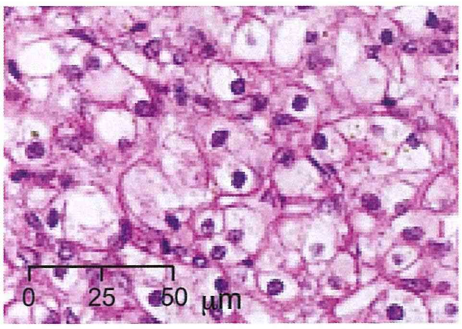

ccRCC-79

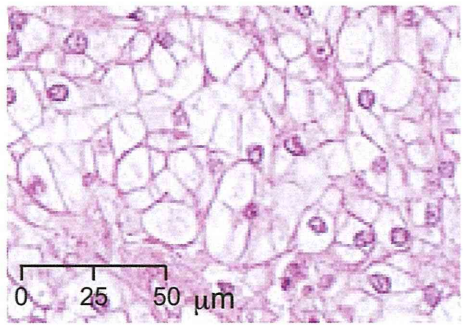

ccRCC-81

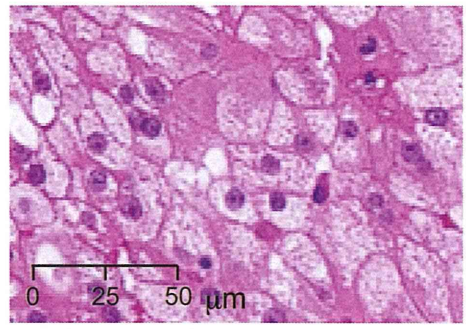

ccRCC-138

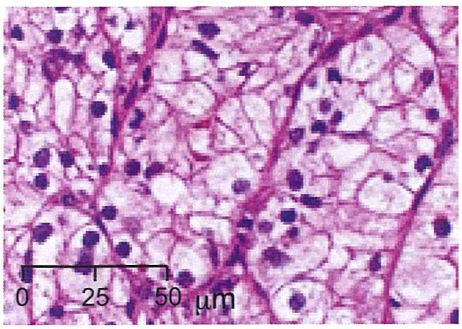

ccRCC-184

Histologies of tumors having no *VHL* or *TCEB1* alterations.
All cases were confirmed as clear cell RCC on HE staining .

Nature Genetics: doi:10.1038/ng.2699

Allogenic Skeletal Myoblast Transplantation in Acute Myocardial Infarction Model Rats

Yukiko Imanishi,[1] Shigeru Miyagawa,[1] Atsuhiro Saito,[2] Satoru Kitagawa-Sakakida,[1,3] and Yoshiki Sawa[1,2,4]

Background. The limitations of syngenic cell therapy include patient safety and quality control of the source cells. Therefore, it is important to develop and assess procedures using allogenic cells. We investigated the impact of allogenic skeletal myoblast (SMB) transplantation on acute myocardial infarction with respect to immune response, donor cell survival, and therapeutic efficacy.

Methods. Female Lewis rats underwent proximal left anterior descending coronary artery ligation. Fifteen minutes later, they underwent major histocompatibility (MHC)-matched Lewis SMB transplantation (group S) and MHC-mismatched ACI SMB transplantation (group A), or treated with buffer injection as a control (group C).

Results. Flow cytometry showed that the SMBs expressed MHC antigens and B7 signal molecules in vitro. In group A, transcription levels of interleukin-2 receptor and interferon-γ were significantly increased 7 days after transplantation, and the area surrounding the donor SMBs was intensely infiltrated with CD4- and CD8-positive cells. Estimation of the number of donor cells in the recipient left ventricular chamber revealed that except for day 0, group A had fewer donor SMBs, which disappeared faster, compared with group S. Echocardiography demonstrated that the ejection fraction (EF) of group A was lower than that of group S.

Conclusion. MHC-mismatched allogenic SMB transplantation in infarcted myocardium induces the immune response and acceleration of donor cell clearance, decreasing the therapeutic effect. Donor cell survival and inflammation may play important roles in the therapeutic mechanism of SMB transplantation therapy for acute myocardial infarction.

Keywords: Allogenic, Cell transplantation, Skeletal myoblast, Donor cell survival, Immune rejection, Acute myocardial infarction.

(*Transplantation* 2011;91: 425–431)

Recently, clinical trials using autologous cell therapy to treat ischemic heart failure have drawn worldwide attention. Randomized, controlled clinical trials have demonstrated that cell therapy is safe and promising, but it is not yet sufficiently effective in recovering cardiac function in patients after myocardial infarction (MI) (*1–4*). Its limitations include potential injury to patients during cell harvesting and the difficulty of obtaining a stable supply of uniform quality cells from patients of various backgrounds. More refinements are needed to use cell therapy effectively in clinical applications, including the use of allogenic cells rather than autologous cells.

Allogenic bone marrow mesenchymal stem-cell (MSC) transplantation is reported to show little immunogenicity and can even exert immunomodulating effects (*5–7*). We also reported that allogenic bone marrow MSC transplantation is feasible and effective for treating acute MI (AMI), partly because of its low immunogenicity (*8*). Skeletal myoblasts (SMBs) are another powerful cell source for treating ischemic heart failure (*9*). For treating Duchenne muscular dystrophy, however, allogenic SMB transplantation has been largely inefficient, because of the host's immune response to the donor SMBs (*10, 11*). There is evidence that the sensitivity of the immune reaction in allogenic transplantation is affected not only by histocompatibility matching but also by the combi-

This work was in part supported by a grant from the Japanese Ministry of Health, Labor and Welfare (Research Grant for Human Genome and Tissue Engineering).

The authors declare no conflict of interest.

[1] Division of Cardiovascular Surgery, Department of Surgery, Graduate School of Medicine, Osaka University, Osaka, Japan.

[2] Medical Center for Translational Research, Osaka University Hospital, Osaka, Japan.

[3] Department of Cardiology, Takarazuka Daiichi Hospital, Hyogo, Japan.

[4] Address correspondence to: Yoshiki Sawa, M.D., Ph.D., Division of Cardiovascular Surgery, Department of Surgery, Graduate School of Medicine, Osaka University, E1 2-2 Yamada-oka, Suita City, Osaka 565-0871, Japan.

E-mail: sawa@surg1.med.osaka-u.ac.jp

Y.I. participated in the writing of the manuscript; S.M. and A. S. participated in the research design; S.K.-S. participated in the data analysis; and Y. S. participated in the research design.

Supplemental digital content is available for this article. Direct URL citations appear in the printed text, and links to the digital files are provided in the HTML text of this article on the journal's Web site (www.transplantjournal.com).

Received 29 July 2010. Revision requested 31 August 2010.

Accepted 3 November 2010.

ISSN 0041-1337/11/9104-425

DOI: 10.1097/TP.0b013e3182052bca

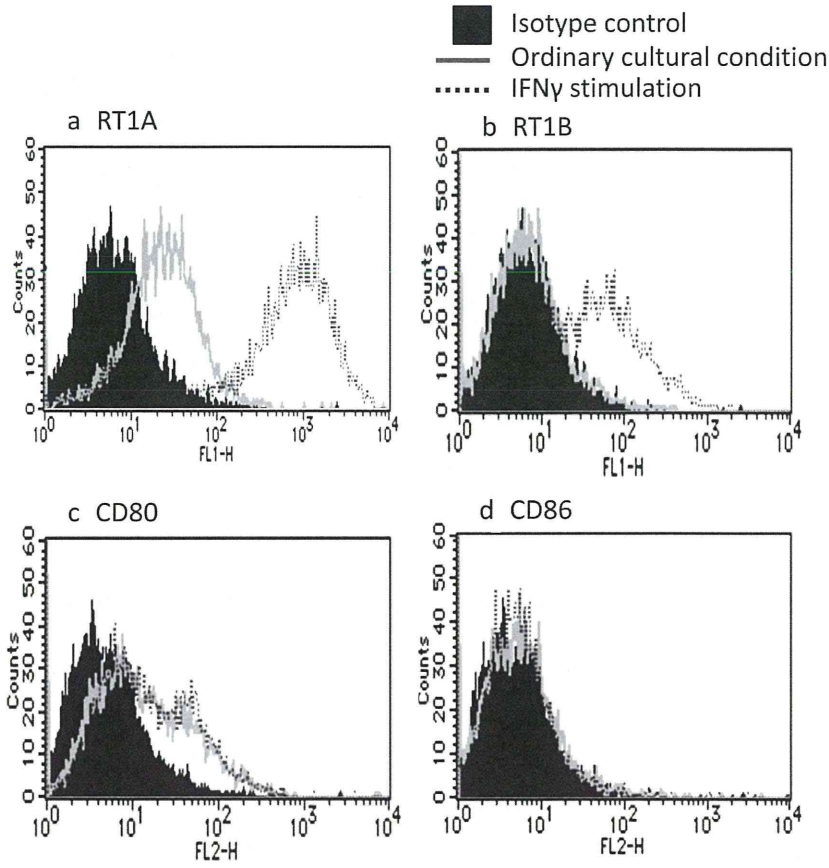

FIGURE 1. Expression of immunologically important cell surface molecules on skeletal myoblasts (SMBs). RT1A (major histocompatibility [MHC] class I), RT1B (MHC class II), CD80 (B7.1), and CD86 (B7.2) were analyzed by flow cytometry. (a) The SMBs were positive for RT1A expression, which was enhanced by interferon (IFN)-γ stimulation. (b) The SMBs were usually negative for RT1B, but they became RT1B positive with IFN-γ stimulation. (c) The cells were positive for CD80. (d) The cells were negative for CD86 regardless of INF-γ stimulation. *Filled curves* show SMBs stained with isotype-matched controls. *Solid-line curves* show SMBs grown under normal culture conditions and stained with each of the antibodies. *Dotted-line curves* show SMBs with INF-γ stimulation and stained with each of the antibodies.

nation of the donor source and transplantation site (*12–15*). For future clinical applications of allogenic SMB transplantation into infarcted myocardium, it is important to evaluate the basal donor cell survival, immune reaction, and therapeutic efficacy. Such studies may also shed more light on the mechanisms underlying its therapeutic effect and indicate ways to improve the therapeutic effect of conventional SMB transplantation therapy.

In this study, our aim was to evaluate the immune reaction after allogenic SMB transplantation into ischemic myocardium and its impact on graft survival and therapeutic effect. We transplanted major histocompatibility (MHC)-mismatched allogenic SMBs into left anterior descending coronary artery-occluded rats without using immunosuppressive drugs and analyzed the immune reaction, donor cell survival, and therapeutic efficacy.

RESULTS

In Vitro Analysis of SMB Immunogenicity

SMBs harvested from 3-week-old ACI and Lewis (LEW) rats were examined for immunity-related cell surface markers by flow cytometry. There were no differences in the marker expressions between the SMB origins of the strains. SMBs expressed the MHC class I molecule RT1A. When SMB immunogenicity was enhanced by interferon (IFN)-γ, the level of MHC class I increased (Fig. 1a). SMBs did not express the MHC class II molecule RT1B under ordinary culture conditions, but they became positive for it under IFN-γ stimulation (Fig. 1b). Furthermore, B7.1 (CD80) was expressed and B7.2 was not, and these expressions were not affected by IFN-γ stimulation (Fig. 1c and d). The SMBs were negative for CD45, indicating that there was no contamination or hematopoietic cell differentiation (data not shown).

Immunoreactions Induced by Allogenic SMB Transplantation in AMI Model Rats

To examine the immune response after allogenic SMB transplantation, the transcription levels of interleukin-2 receptor (IL-2R) and IFN-γ, which reflect the level of activated T-cell infiltration, were measured in recipient hearts using quantitative reverse-transcriptase polymerase chain reaction (PCR; Fig. 2). On day 7, group A showed significantly higher IL-2R expression than groups C and S, and it was still higher on day 28 (Fig. 2a). The IFN-γ expression also indirectly reflects the level of immune rejection. The changes in IFN-γ expression in group A coincided with the IL-2R expression pattern, which was significantly increased on days 7 and 28 compared with group C. In group S, IFN-γ increase was also observed on days 7 and 28 (Fig. 2b).

Infiltration of T Cells Into the Cell Transplantation Area

Immunohistochemical analysis was performed 7 days after SMB transplantation, when the transcription levels of

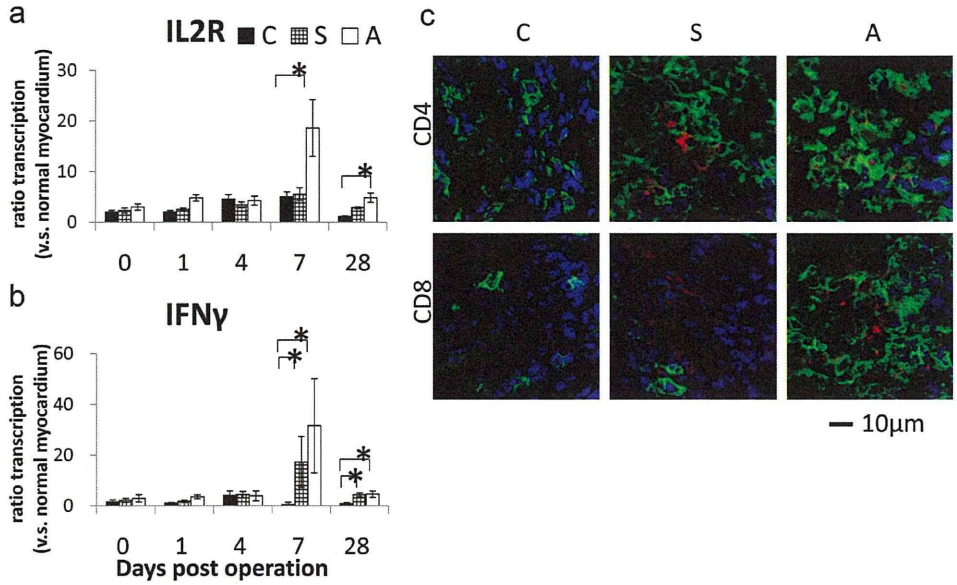

FIGURE 2. Evaluation of the immune response in recipient hearts. Transcriptional levels of (a) interleukin-2 receptor (IL-2R) and (b) interferon (IFN)-γ in recipient hearts 0, 1, 4, 7, and 28 days after transplantation were determined by quantitative reverse-transcriptase polymerase chain reaction assays. The values were normalized to the endogenous control GAPDH and represented as a ratio to the transcription level in normal myocardium. (a) In group A, the level of IL-2R was significantly increased 7 and 28 days after transplantation compared with groups C and S. (b) The IFN-γ level showed a similar pattern of transition to that of IL-2R. In group A, IFN-γ was increased 7 and 28 days after transplantation. *Filled columns* show group C, *checkered columns* show group S, and *open columns* show group A. *P less than 0.05. (c) T-cell infiltration into the cell transplantation area. Representative images from each group are shown. The level of CD4-positive cell infiltration was the same between groups S and A and increased compared with group C (*upper*). The infiltration of CD8-positive cells was especially enhanced in group A (*lower*). *Blue*: nuclei, *red*: implanted skeletal myoblasts, and *green*: CD4 or CD8. Bar=10 μm.

IL-2R and IFN-γ were significantly increased. A strong infiltration of CD4-positive T cells was observed around the donor SMBs of groups A and S compared with group C (Fig. 2c, upper). In contrast, many more infiltrated CD8-positive T cells were observed in group A than in groups S and C (Fig. 2c, lower).

Time Course Analysis of Donor Cell Number in Infarcted Left Ventricle

We evaluated the number of donor cell survival in the recipient myocardium by quantitative PCR for donor-specific *sry* gene and calculated from a standard curve. In group C, no specific signals for *sry* were detected at any time point. Fifteen minutes after transplantation, 0.5×10^6 or fewer cells were detected in groups S and A, which was approximately 10% of the prepared donor cells. In group A, the number of initially delivered donor cells was the same as in group S. Thereafter, the number of allogenic SMBs was lower in group A than in group S; half of the donor cells in group A disappeared within 7 days, and no cells were detected 28 days after transplantation (Fig. 3a). In group S, the donor cells proliferated nearly 5-fold from day 1 to 4, then decreased thereafter. Cell proliferation at day 4 was also confirmed by bromodeoxyuridine incorporation (see **Figure, Supplemental Digital Content 1,** http://links.lww.com/TP/A337). At 28 days after transplantation, the number of residual donor cells in the infarcted heart tissue in group S was nearly half of the initial count.

Detection of Donor Cells in Recipient Hearts

We performed histologic analyses 4 days after transplantation to identify the donor cells. In group S, large numbers of donor SMBs were detected in the scar area and in the border zone between the scar and normal areas (Fig. 3b and c). In group A, only a few donor SMBs were detected compared with group S (Fig. 3f and g), which confirmed the PCR findings (Fig. 3a). The donor cells had a fibroblastic shape but were not cardiomyocytes and did not have a capillary component (Fig. 3d and e).

Echocardiography Findings After Allogenic SMB Transplantation in AMI Model Rats

Cardiac performance was determined 8 weeks after cell transplantation using echocardiography (Fig. 4). There were no significant differences for body weight, heart rate, or blood pressure among the experimental groups (data not shown). The left ventricular (LV) end-diastolic dimension (Fig. 4a) and LV end-systolic dimension (LVDs; Fig. 4b) were not significantly different among the three groups, although the LVDs in group S was relatively small ($P=0.067$ vs. group A; Fig. 4b). The LV ejection fraction, which represents contractility, was calculated from the LV end-diastolic dimension and LVDs. The LV ejection fraction value in group A was the same as in group C, whereas it was significantly higher in group S (Fig. 4c).

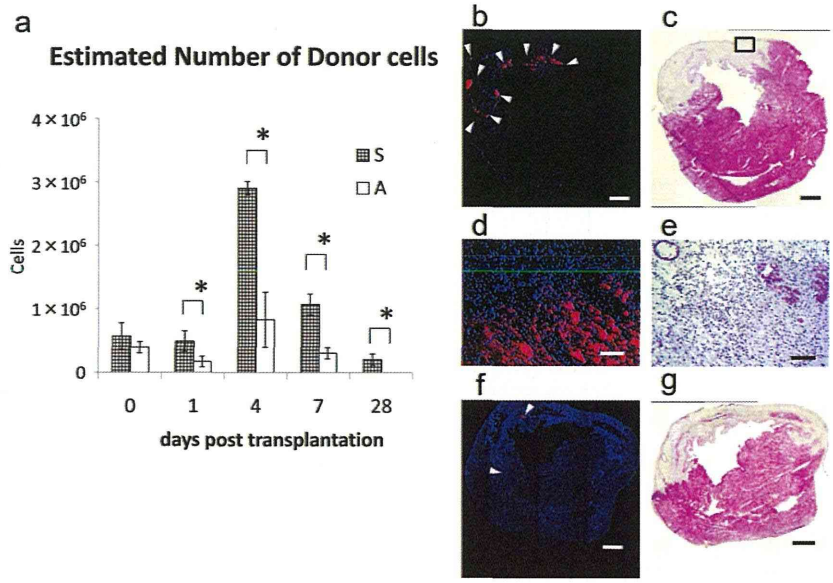

FIGURE 3. Detection of donor skeletal myoblasts (SMBs) in recipient hearts. (a) The number of donor cells was significantly lower in group A than in group S on days 1, 4, 7, and 28. *Checkered columns* show group S, and *open columns* show group A. **P* less than 0.05. (b–g) Recipient hearts were analyzed by histology 4 days after PKH26-labeled SMB transplantation. (b) In group S, abundant SMBs were detected. (c) Serial section of the image in b, showing that most of the donor cells were surrounded by infarcted area. (d and e) High-magnification images of the *square* in c, showing the surviving donor cells with a fibroblastic shape. (f) Fewer donor cells were detected in group A than in group S. (g) Serial section of the image in f showing donor cells surrounded by infarcted area. (b–e) Group S; (f and g) group A; (b, d, and f) 6-diamidino-2-phenylindole staining; and (c, e, and g) hematoxylin-eosin staining. *Blue*: nuclei, *red*: fluorescent dye-labeled donor SMBs. *Arrowheads*: donor SMBs. (b, c, f, and g) Bar=1 mm and (d and e) Bar=100 μm.

DISCUSSION

In this study, we evaluated allogenic SMB transplantation in AMI model rats with a focus on the implanted cell survival and immune response. SMBs potentially expressed both MHC and B7 signal molecules (Fig. 1), which suggested that allogenic SMBs might be targeted by the host's immune response. Indeed, our in vivo analyses showed increased IL-2R and IFN-γ transcription in the recipient myocardium tissues (Fig. 2a and b). Seven days after transplantation, the IL-2R and IFN-γ expressed by immunocytes were notably increased in group A, indicating that a higher level of inflammation with immune rejection was induced by allogenic than by syngenic SMB transplantation. In addition, histologic analysis showed that the grafted allogenic SMBs were surrounded by CD4- and CD8-positive T cells (Fig. 2c, right). Immune rejection may also affect the donor cell clearance rate. There were fewer allogenic SMBs in the recipient hearts than syngenic ones, and their number decreased over time, disappearing within 28 days, when syngenic SMBs still remained (Fig. 3a). Histologic analysis of the transplanted labeled SMBs showed that the allogenic SMB aggregates were small and sparse compared with those of the syngenic SMBs (Fig. 3b–g). The higher inflammation level and lower rate of donor cell survival may indicate a loss of therapeutic benefit from allogenic cell transplantation for AMI (Fig. 4). This is the first report to estimate the number of implanted allogenic and syngenic SMBs and to assess the immune reaction in the infarcted myocardium over time.

Both the innate and adaptive immune systems are implicated in the destruction of allogenic cells. Both syngenic and allogenic transplanted cells are destroyed by the innate immune system shortly after cell transplantation. Then $CD4^+$ and $CD8^+$ T cells infiltrate locally around the alloantigens. As shown by flow cytometry analysis, the SMBs expressed both MHC class I and costimulatory signal molecules (Fig. 1). $CD4^+$ and $CD8^+$ T cells activated by antigens of the allogenic SMBs may mediate the immunologic rejection. Guo et al. (*16*) demonstrated that allogenic SMB transplantation at 1 week after MI had a comparable effect to autotransplantation when an immunosuppressive reagent was used. In allogenic SMB transplantation for MI, modulation of the immune responses and prolong donor cell survival by immunosuppressive reagents usage or gene modification of donor SMBs may be a strategically effective approach.

An increase in IFN-γ at the transcriptional level, and CD4-positive cell infiltration, was observed in group S at 7 days after transplantation. Although we used LEW rats for both the donors and recipients in our syngenic transplantation model, a T-cell response was still observed. This response is directed against minor histocompatibility antigens (*17*, *18*). In particular, the male-specific H-Y antigen from a donor is known to induce an immune response in female recipients, mainly by CD4-positive T-cell activation (*17*, *19*). Sakakida et al. (*20*) reported that sex-mismatched skin grafts in LEW rats survive, which suggests that the H-Y antigen is not so critical in transplantations between LEW rats. We performed sex-mismatched transplantation to quantify the male donor cells in female recipient hearts. Our findings support the idea that major and minor histocompatibility-matched

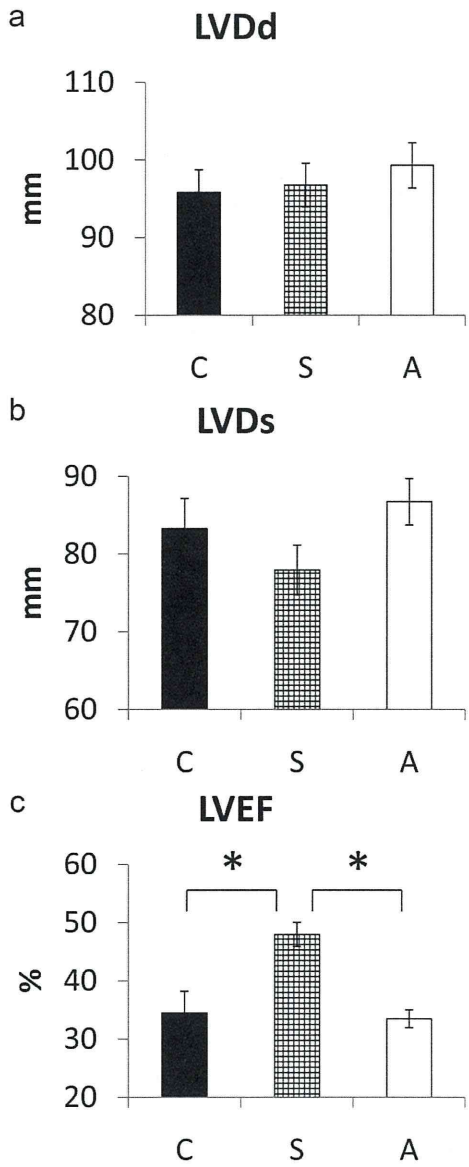

FIGURE 4. Evaluation of cardiac performance. (a) The left ventricular end-diastolic dimension (LVDd) and (b) left ventricular end-systolic dimension (LVDs) were determined by echocardiography 8 weeks after cell transplantation. (c) The left ventricular ejection fraction (LVEF) was calculated as LVEF(%)=(LVDd^3−LVDs^3)/LVDd^3×100. The positive control, group S, showed a lower LVDs and higher LVEF compared with group C, whereas group A did not show any differences from group C. *Filled columns*, group C; *checkered columns*, group S; and *open columns*, group A. *P less than 0.05.

transplantation might improve the therapeutic effect by minimizing the immune response.

We observed a strong immune reaction and low donor integration in group A, which were associated with a loss of therapeutic benefit. These findings have implications for the mechanisms involved in SMB transplantation therapy for MI. In MSC transplantation therapy for AMI, paracrine factors may function as the main regulators, and donor cell survival might not be so important (*21*). In addition, some reports have suggested the contribution of soluble factors in SMB transplantation (*22–26*). Farahmand et al. (*24*) reported that the beneficial effect of SMB transplantation is because of the inhibition of matrix remodeling in noninfarcted tissue, which is probably mediated by a paracrine effect. However, it seems unlikely that the therapeutic gain in SMB transplantation is entirely due to a paracrine effect. In this study of SMB transplantation, the donor cells were much more abundant and survived for a longer period (Fig. 3), compared with MSC transplantation. We previously evaluated the number of MSC in infarct myocardium using the same technique (*8*). The number of syngenic MSC in infarct myocardium decreased notably within the first 24 hr and then continued to decrease slowly, although it was effective. Conversely, even in allogenic SMB transplantation, this number was higher compared with syngenic MSC (day 1: $1.71\times10^5\pm84617$ vs. $4.52\times10^4\pm13061$). In SMB transplantation therapy, it is possible that the grafted SMB themselves contribute directly to reduce wall stress, increase scar elasticity, and buttress infarcted LV walls, which would limit LV remodeling (*9*). Although controversy remains, it was also reported that SMBs in infarcted myocardium differentiate into a myogenic lineage and compensate for lost contractile ability (*27*). The low level and short-term existence of allogenic SMBs in the myocardium may thus relate to the absence of a therapeutic effect.

The number of donor SMBs was increased on day 4 after transplantation (Fig. 3). Some reports have noted that grafted SMBs proliferate in both infarcted and noninfarcted myocardium (*28*, *29*). Furthermore, we previously reported that MSCs do not proliferate (*8*). These findings may indicate differences in the skeletal muscle cell properties, which potentially have a greater tolerance than other cell types to hypoxic conditions (*29*). The donor SMBs began to decline on day 7 (Fig. 3), which correlated with the activation of the immune response (Fig. 2). In addition, the donor cells disappeared in group A, in which a stronger and more rapid immune response occurred than in group S, strongly suggesting that the disappearance of donor cells is influenced by their immunogenicity.

In summary, in a rat model of infarcted myocardium, MHC-mismatched allogenic SMB transplantation induced an immune response with CD4- and CD8-positive T-cell activation; this response was associated with accelerated donor cell clearance and loss of therapeutic effect. Furthermore, our findings suggest that donor cell survival and inflammation are important aspects of the therapeutic mechanism of SMB transplantation for AMI, although additional investigation is needed.

MATERIALS AND METHODS

Humane animal care was performed in compliance with the "Principals of Laboratory Animal Care" formulated by the National Society for Medical Research and the "Guide for the Care and Use of Laboratory Animals" prepared by the Institute of Laboratory Animal Resources and published by the National Institutes of Health (NIH publication No. 85-23, revised 1996).

SMB Harvest and Culture

SMBs were harvested from the tibialis anterior muscle tissues of 3-week-old ACI (ACI/NJcl: RT-1^{av1}, CLEA Japan, Inc., Tokyo, Japan) and LEW

TABLE 1. Primers and probes used in this study

	Forward primer	Reverse primer	Probe
IL-2	GCCTTGTGTGTTATAAGTAGGAGGC	AGTGCCAATTCGATGATGAGC	TCTCCTCAGAAATTCCACCACAGTTGCTG
SRY	GCCTCAGGACATATTAATCTCTGGAG	GCTGATCTCTGAATTCTGCATGC	AGGCGCAAGTTGGCTCAACAGAATCC
GAPDH	CCATCACTGCCACTCAGAAGAC	TCATACTTGGCAGGTTTCTCCA	CGTGTTCCTACCCCCAATGTATCCGT
IL-2R	CCCTCAGGTGTTTCTTGAGCTT	CTTTCCCAGAGAGTGAGGCTTC	TGGCCACTGCTACCTGATACTCCTTTGTGA
IFN-γ	ATCGAATCGCACCTGATCACTA	TTCTTATTGGCACACTCTCTACCC	AACAACCCACAGATCCAGCACAAAGC

IL-2R, interleukin-2 receptor; IFN, interferon.

(LEW/Sea: RT-1^l, Kyudo, Kumamoto, Japan) rats, as described previously (*30*). Briefly, cells from the muscle mass were obtained by enzymatic dissociation, by adding 0.2% collagenase type II (Life Technologies, CA) and shaking vigorously for 1 hr at 37°C. The extracts of muscle cell were then preplated in collagen-coated flasks (BD, NJ). Twenty-four hours after isolation, the nonadherent cell suspension was collected and seeded on Matrigel (0.5 mg/mL; BD)-coated flasks and allowed to attach for the next 48 hr. SMBs were grown in Dulbecco's modified Eagle's medium (D-MEM; Life Technologies) containing 20% heat-inactivated fetal bovine serum (lot selected for promoting rapid SMB expansion; MP Biochemicals, LLC, CA), 2 mM L-glutamine (Life Technologies), and penicillin streptomycin (Life Technologies) at 37°C and 5% CO_2 for 7 days. To identify implanted cells in vivo, SMBs were labeled using a PKH26 red fluorescent linker kit (Sigma-Aldrich Corp., MO) at the end of culture, following the manufacturer's instructions. To enhance SMB immunogenicity, SMBs were pretreated with 10 ng/mL recombinant rat IFN-γ (Wako Pure Chemical Industries, Ltd., Osaka, Japan) for 4 days before use (*31*).

Animal Experiments

LEW rats were prepared as a model of acute heart failure and placed randomly into three treatment groups: those that underwent transplantation of LEW SMBs (syngenic SMB transplantation: group S), those that underwent transplantation of ACI SMBs (allogenic SMB transplantation: group A), and those that underwent cell-free buffer injection, as the no-treatment control (control: group C). Twenty-five rats in each group were used for DNA and RNA preparations at 0 (15 min), 1 (24 hr), 4, 7, and 28 days after transplantation (five rats at each time point). Six rats in each group were used for histologic analysis at 4 and 7 days after transplantation (three at each time point), whereas 10 rats in each group were examined by echocardiography 8 weeks after transplantation.

Eight-week-old female LEW rats weighing 150 to 180 g were used as SMB recipients. MI was produced by ligation of the left anterior descending coronary artery, as described previously (*32*), then subjected to cell transplantation 15 min later. A suspension of SMBs (5.0×10^6 in 200 μL of Hank's buffered salt solution; Sigma-Aldrich) obtained from a male ACI or LEW rat, or 200 μL of cell-free Hank's buffered salt solution, was injected into the LV anterior wall of heart of each recipient female rat at five points, using a 26-gauge needle. Injection was performed under direct observation with a surgical microscope to ensure there was no leakage of the cell suspension. If leakage was suspected, the sample was excluded from the study. The rats were allowed to recover under care.

The recipient rats were killed at 0 (15 min), 1 (24 hr), 4, 7, and 28 days after surgery by intravenous injection of pentobarbital (200 mg/kg body weight; DS Pharma Biomedical Co., Ltd, Osaka, Japan) and potassium chloride (30 mM; Wako Pure Chemical Industries) to cause cardiac arrest in diastole under terminal anesthesia, and the heart was excised. Hearts used for *sry* gene and RNA analyses were dissected to remove the right ventricular free wall and soaked in RNA Later (Qiagen, Hilden, Germany). Hearts used for histologic examinations were cut into three segments, embedded in optimal cutting temperature (OCT) compound (Sakura Finetek Japan Co., Ltd., Tokyo, Japan), and snap-frozen in liquid nitrogen.

Measurement of Donor Cell Number

The procedure used to determine the number of donor cells in the recipient hearts was described previously (*8*, *20*). The number of donor SMBs was determined at 0 (15 min), 1 (24 hr), 4, 7, and 28 days after transplantation. Quantitative PCR assays for *sry* and *IL-2* were performed with the primers and probes listed in Table 1. The probes were labeled with a 5′ fluorogenic probe (6-carboxyfluorescein [6FAM]) and a 3′ quencher (5/6-carboxy-tetramethyl-rhodamine [TAMRA]).

Histologic Analysis

Histologic analyses were performed at 4 and 7 days after transplantation. The hearts were cut transversely from the apex to the base into three equal slice samples and frozen in liquid nitrogen. These frozen samples were cut into 5-μm cryosections. To evaluate T-cell infiltration into the border zone, the sections from day 7 were stained with antibodies for CD4 and CD8 (1:100 dilutions, Millipore, MA). The second antibody was Alexa488-conjugated goat anti-mouse antibody (1 μg/mL, Life Technologies). The samples were then counterstained with 6-diamidino-2-phenylindole (1 μg/mL, Dojindo Laboratories, Kumamoto, Japan). To identify implanted cells, which had been labeled with fluorescent dye, the sections from day 4 were stained with 6-diamidino-2-phenylindole or hematoxylin-eosin and examined by fluorescence microscopy (Keyence Corp., Osaka, Japan) and confocal microscopy (Bio-Rad Laboratories Inc., CA).

Statistical Analysis

All values are expressed as the mean±standard error of the mean. To assess the significance of differences between individual groups, statistical evaluations were conducted using one-way analysis of variance with Fisher's protected least significant difference (PLSD). *P* less than 0.05 was considered significant.

An expanded Materials and Methods section is available as **Supplemental Digital Content 2** (http://links.lww.com/TP/A338).

ACKNOWLEDGMENTS

The authors thank Masako Yokoyama for excellent technical assistance. They also thank all the members of the Cardiovascular Surgery Laboratory of Osaka University for helpful discussions.

REFERENCES

1. Herrmann JL, Abarbanell AM, Weil BR, et al. Cell-based therapy for ischemic heart disease: A clinical update. *Ann Thorac Surg* 2009; 88: 1714.
2. Menasche P, Alfieri O, Janssens S, et al. The Myoblast Autologous Grafting in Ischemic Cardiomyopathy (MAGIC) trial: First randomized placebo-controlled study of myoblast transplantation. *Circulation* 2008; 117: 1189.
3. Schachinger V, Assmus B, Erbs S, et al. Intracoronary infusion of bone marrow-derived mononuclear cells abrogates adverse left ventricular remodelling post-acute myocardial infarction: Insights from the reinfusion of enriched progenitor cells and infarct remodelling in acute myocardial infarction (REPAIR-AMI) trial. *Eur J Heart Fail* 2009; 11: 973.
4. Meyer GP, Wollert KC, Lotz J, et al. Intracoronary bone marrow cell transfer after myocardial infarction: Eighteen months' follow-up data from the